

Nonlinear behaviour of neural networks with dynamical thresholds

This article has been downloaded from IOPscience. Please scroll down to see the full text article.

1995 J. Phys. A: Math. Gen. 28 1335

(<http://iopscience.iop.org/0305-4470/28/5/019>)

View [the table of contents for this issue](#), or go to the [journal homepage](#) for more

Download details:

IP Address: 171.66.16.68

The article was downloaded on 02/06/2010 at 01:11

Please note that [terms and conditions apply](#).

Nonlinear behaviour of neural networks with dynamical thresholds

N Lemke†§, J J Arenzon†||, R M C de Almeida†¶ and S Goulart Rosa Jr‡+

† Instituto de Física, Universidade Federal do Rio Grande do Sul, CP 15051–9150-970, Porto Alegre, RS, Brazil

‡ Instituto de Física de São Carlos, CP 369–13560-970, São Carlos, SP, Brazil

Received 12 July 1994

Abstract. A dynamical system of coupled neurons with variable thresholds is solved analytically and compared with numerical simulations. The system behaviour is extremely rich presenting intermittence, chaos, crises etc depending on the parameters.

1. Introduction

Many authors [1] have emphasized the relevance of the chaotic behaviour present in natural neural systems like the human brain to the understanding of their striking features such as creativeness, complex interactions among memories, etc. Most neural network models based on the Hopfield model present very simple dynamics comprising only fixed points which, although suitable for pattern retrieval, do not give adequate behaviour in some contexts since a never stopping path on the phase space is a characteristic of living brains. To circumvent this difficulty new ingredients had to be added to the Hopfield recipe, such as high order [2] or asymmetric connections [3], time delays [4], dynamical thresholds [5, 6], etc. In this paper we extend the study of a recent simple model proposed by Moreira and Auto [6] that presents complex behaviour using dynamical thresholds to analyse and highlight the role of complex dynamics in neural networks. Chaos and intermittency may arise in such systems: the chaotic behaviour being characterized by the presence of a non-periodic attractor along with sensitivity to initial conditions while the intermittency signature consists of abrupt bursts during laminar behaviour of the dynamical variable.

There is biological evidence that neural thresholds are not static and may vary depending on the past history of a given neuron. When introduced, dynamical thresholds normally generate a rich behaviour. Horn and Usher [5] used a biologically inspired threshold rule and, when studying a network with only one pattern embedded, found an oscillating phase besides the usual ordered and disordered ones. When several patterns are embedded, the system exhibits transitions and may oscillate from one memory to another.

Recently, Moreira and Auto [6] simulated networks with a low degree of connectivity (each neuron is connected with only ten neighbours) using the following rule for the

§ E-mail address: lemke@ifl.ufrgs.br

|| E-mail address: arenzon@ifl.ufrgs.br

¶ E-mail address: rita@ifl.ufrgs.br

+ E-mail address: sgrasa@ifqsc.anp.br

threshold evolution:

$$\Theta(t+1) = \Theta(t) - \frac{p}{|\Theta(t)|} + qa(t) \quad (1)$$

where p and q are tunable parameters and the threshold is the same for all neurons. The quantity $a(t)$ is the network activity defined as the fraction of firing neurons:

$$a(t) = \frac{1}{N} \sum_{i=1}^N S_i(t) \quad (2)$$

where $S_i(t)$ is the state of the i th neuron at the instant t and may assume the values 0 (latent) or 1 (active).

The noise-free dynamics is defined as

$$S_i(t+1) = \frac{1}{2}[1 + \text{sgn}(h_i(t) - \Theta(t))] \quad (3)$$

where the local field acting on the i th neuron is the weighted sum of incoming signals

$$h_i(t) = \sum_{j \in C_i} J_{ij} S_j \quad (4)$$

and J_{ij} are the synaptic connections and C_i is the cluster of neurons connected to i . The network studied by Moreira and Auto [6] had no previous learning and the connections are randomly chosen in the interval $[-1, 1]$.

The role played by the above dynamical threshold is nonlinear in character and analytical calculation is welcome. Here we use a slightly different version that considers discrete ± 1 synapses sorted with the same probability. We checked that besides making the analytical expressions simpler, this does not introduce any qualitative change in the model in the sense that the chaotic/intermittent behaviour remains the same although there are some quantitative differences. These ± 1 connections are not equivalent to having only one pattern embedded via the Hebb rule because in that case the connections would be separable and any average over the synapses in a closed loop would be positive implying that the model could be mapped to a non-frustrated ferromagnet. The model using the Hebb prescription for the synapses is being studied and will be published elsewhere.

2. The analytical solution

Dilution in the synaptic connections has been introduced in numerous models of neural networks for several reasons; besides being more realistic biologically, such models turn out to have an exactly solvable dynamics in the limit of high dilution where annealing averages apply exactly [7]. Recently, Arenzon and Lemke [8] showed that reliable simulations of such systems may be performed with results agreeing successfully with the available theoretical predictions.

The activity at a given time can be obtained as a function of the activity in the previous time step:

$$a(t+1) = \frac{1}{2}[1 + \langle \langle \text{sgn}(h_i(t) - \Theta(t)) \rangle \rangle_{J,S}] \quad (5)$$

where $\langle \langle \rangle \rangle_{J,S}$ denotes the average over the connections and over the possible network states. These averages can be easily evaluated observing that if the system has activity a at a given time, in the next time step the probability of having $J_{ij} S_j$ are given by

$$J_{ij} S_j = \begin{cases} +1 & \text{with probability } a/2 \\ 0 & 1-a \\ -1 & a/2 \end{cases} \quad (6)$$

and the evolution of the activity is ruled by

$$a(t + 1) = \frac{1}{2} \sum_{n=0}^C \sum_{m=0}^n \binom{C}{n} \binom{n}{m} \frac{(1 - a(t))^{C-n} a^n(t)}{2^n} [1 + \text{sgn}(n - 2m - \Theta(t))] \quad (7)$$

where C is the connectivity of each neuron.

The above fixed connectivity dynamics can be easily extended to the cases where there is thermal noise in the system or when the connectivity is not kept constant.

3. Results

When the threshold given by (1) is allowed to be a dynamical variable many interesting new features are introduced that deserve attention. Since in this case the model presents a very complex behaviour, we first considered the situations where either the activity or the threshold are constant before coupling the maps $a(t)$ and $\Theta(t)$.

3.1. The one-dimensional maps

We studied the one-dimensional map $\Theta(t + 1) = f(\Theta(t))$, where f is given by

$$f(\Theta(t)) = \Theta(t) - \frac{p}{|\Theta(t)|} + c \quad (8)$$

where c is a constant.

Since the map is not defined at the origin (see figure 1), there are two separate branches, one for $\Theta < 0$ and another for $\Theta > 0$. At each branch there is a fixed point at $\Theta_{\pm} = \pm p/c$, respectively. The stability analysis shows that Θ_+ is stable for $-c^2/2 < p < 0$ while Θ_- is stable for $p > c^2/2$.

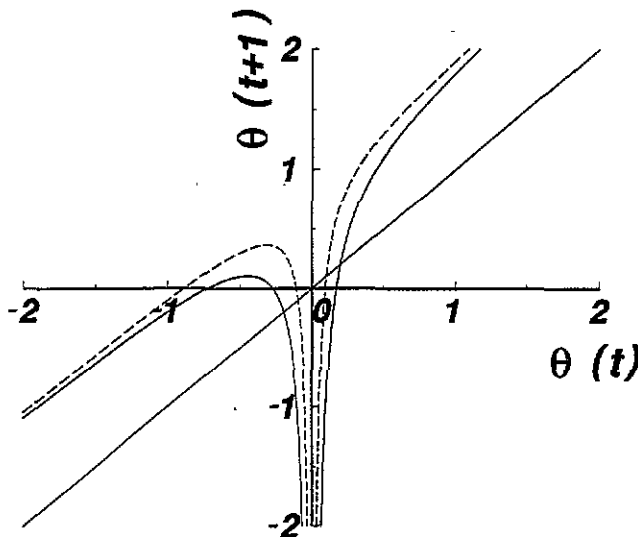


Figure 1. The plot of $\Theta(t + 1)$ versus $\Theta(t)$ for the decoupled one-dimensional situation with $c = 1$. The full curve is for $p = 0.2 < p_c$ while the dashed one is for $p = 0.1 < p_c$. The 45° line is also shown to indicate the unstable and stable fixed points (at the positive and negative branches, respectively).

For $p > c^2/2$ the system settles down in the fixed point $-p/c$ if the initial condition obeys $\Theta(0) < p/c$. As the parameter p decreases, the system follows the period bifurcation route to chaos until the chaotic attractor collides with the unstable orbit $\Theta_+ = p/c$ at $p_c = c^2(1 - \sqrt{2})^2$ when the attractor is suddenly destroyed. This phenomenon is called a boundary crisis.

A crisis is a qualitative change of behaviour that occurs when the chaotic attractor collides with an unstable periodic orbit or with its stable manifold. When the unstable orbit is the boundary of the basin of attraction of the chaotic attractor, the crisis is denominated as a boundary crisis opposed to the interior crisis that happens when the collision occurs inside the basin of attraction. In general, boundary crises destroy the chaotic attractor while interior crises expand it [10].

To obtain the value of p at which the crisis occurs, p_c , we observe that the upper boundary of the chaotic attractor is defined by the relative maximum of the negative branch of the map, $f_{\max} = f(\Theta = -\sqrt{p})$. When f_{\max} equals the unstable fixed point on the positive branch, $\Theta_+ = p/c$, the chaotic attractor is destroyed. For values of p just below the crisis, there is a chaotic transient: Θ wanders in the region previously occupied by the chaotic attractor and, after some steps, goes to infinity. As p approaches p_c from below, the transient time diverges as $|p - p_c|^{-\gamma}$ where γ is the crisis exponent. To estimate γ we first notice that there is an interval around the maximum of the negative branch that, for $p > p_c$, lays above the fixed point on the positive branch and, once attained, injects the system in the divergent region. The interval length is proportional to $|p - p_c|^{1/2}$ and a rough estimation of the mean transient time following Grebogi *et al* [11] is obtained noticing that it is proportional to the inverse of the size of the interval and so scales as $|p - p_c|^{-1/2}$. This value, $\gamma = \frac{1}{2}$, agrees with the one obtained numerically.

For $0 < p < p_c$, the system diverges towards $\pm\infty$ depending whether the value of c is positive or not.

The behaviour observed in the one-dimensional map, equation (8), where the activity is held constant, is also reflected in the behaviour of both maps when they are coupled. However, some novel features are generated in this situation, as for instance, an intermittent behaviour that exists for low values of p due to the appearance of the reinjection mechanism.

The one-dimensional map for the activity $a(t)$ was also studied for constant values of Θ . Differently from the previous case, this map only presents fixed points. For large values of Θ , the fixed point is $a^* = 0$ while it is $a^* = 1$ if Θ is low enough. The transition from $a^* = 1$ to $a^* = 0$ is made through discontinuous steps (where a remains constant) at integer values of Θ .

3.2. The two-dimensional case

When both $\Theta(t)$ and $a(t)$ are coupled, the nonlinearity present in the map of the dynamical threshold originates new features that are not found in the one-dimensional case (several crises, intermittency, etc). In order to study the coupled situation, we extend the scheme developed in [9] for continuous flows.

Given a two-dimensional coupled map described by

$$x_i(t + 1) = F_i(\{x_i\}) \quad i = 1, 2 \quad (9)$$

where the functions $F_i(x, y)$ are not necessarily continuous (but have at most a finite number of discontinuities), the (x_1, x_2) plane can be divided in several regions depending on whether $x_i(t + 1)$ is greater or lower than $x_i(t)$. These regions are called \mathcal{M} and \mathcal{N} for $i = 1$ and 2 , respectively. We are now interested in the one-dimensional boundaries of these regions,

$\partial\mathcal{M}$ and $\partial\mathcal{N}$ and in the points where they cross, $\partial\mathcal{M}\cap\partial\mathcal{N}$ (called vertices). For continuous F_i all the vertices are fixed points of the system (and we call them 'fixed vertices') and orbits whose initial states are close enough will spiral inwards if the fixed point is asymptotically stable. This may not be the case if any of the functions F_i are discontinuous because there may exist points belonging to $\partial\mathcal{M}\cap\partial\mathcal{N}$ that are not fixed points (since these vertices lay in the region where there is a discontinuity, we call such vertices 'jump vertices'). In this latter case, the evolution of an initial state that starts close to one vertex is expelled or at most rotates around it but never converges towards the point.

The vertices location for the coupled maps, equations (1) and (7) may be seen in figure 2(a) for $q = 1$ and $p = 0.2, 0.6$. The full curve is the boundary for the a equation and the other ones are the boundaries for Θ (given by $a = p/q|\Theta|$). When both curves meet we have the vertices of the coupled two-dimensional case. For $p = 0.2$ there are two fixed vertices and one jump vertex. For $p = 0.6$ there are no fixed vertices but one jump vertex; at large enough values of p the positive vertex disappears. When it exists and is a fixed point, it is unstable. Figure 2(b) shows a jump vertex and the boundaries of the four possible regions for a two-dimensional situation. In each region we indicate if the dynamical variables are increasing or not and the evolution of an initial state starting at one of the regions may be easily followed.

The overall system behaviour is shown in figure 3 where diagrams for both Θ and a are plotted as a function of p . There are several important differences from the one-dimensional case that will be detailed below.

Analogously to the one-dimensional case, here there is also a crisis when the chaotic attractor collides with the unstable periodic orbit. However, the crisis occurring at $p_c \simeq 0.054$ (for $q = 1$) is an interior one: there is no other attractor of the dynamics and the unstable fixed point is no longer the boundary of the basin of attraction as in the previous situation. This change of behaviour from a boundary crisis in the one-dimensional case to an interior one when we have a two-dimensional system is also seen in the Hénon map [11]. Usually, in interior crises, for some time the system remains in the region previously occupied by the destroyed attractor before being injected in the new allowed region. Apparently this is not what happens here: below the point where

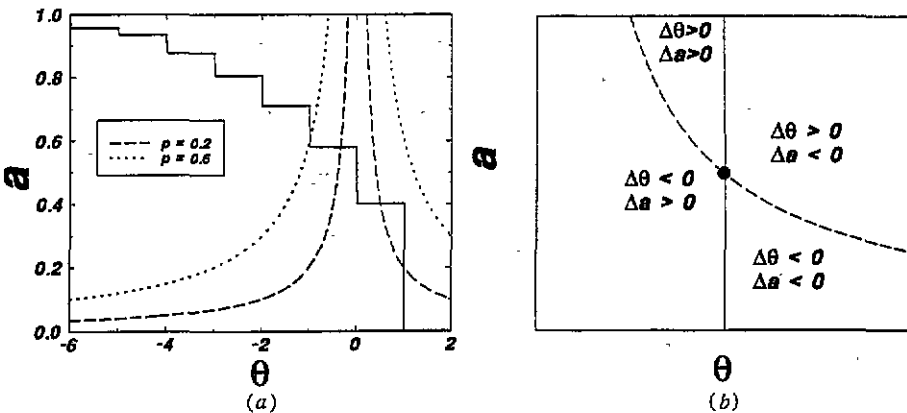


Figure 2. (a) Vertices of the two-dimensional coupled maps (intersections of both curves). The full curve is the boundary for a and the dashed ones are the boundaries for Θ . (b) Jump vertex (full circle) and the boundaries of the four possible regions around it. The behaviour of each dynamical variable is indicated.

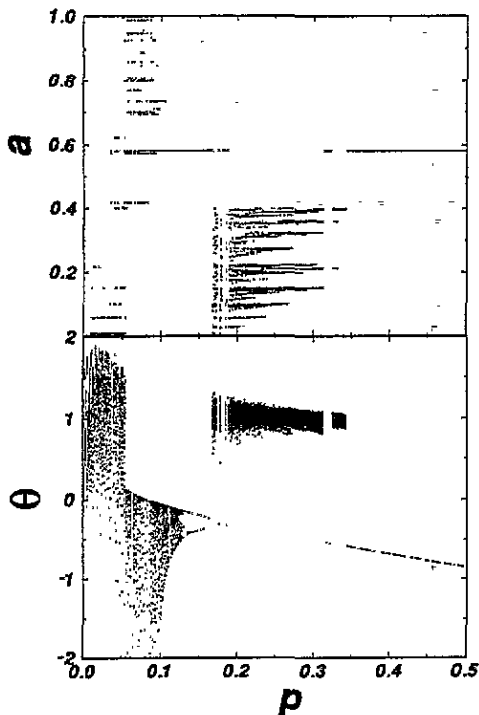


Figure 3. Bifurcation diagrams for Θ and a . Below $p_c \simeq 0.054$ the system is intermittent while above p_c it may be chaotic, suffering an inverse bifurcation cascade until attaining the fixed point. Depending on the initial condition the system may be trapped in the second chaotic attractor.

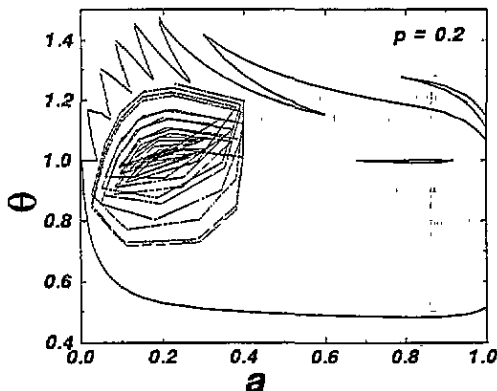


Figure 4. Basin of attraction of the chaotic attractor coexisting with the fixed point for $p = 0.2$. This basin is disjoint and presents islands (at least one) from where the fixed point is reached.

the crisis occurs, the system is no longer chaotic but intermittent although the dynamical variables may assume values that are not in the region defined by the remnants of the late attractor.

For increasing values of p (above p_c) the system suffers an inverse bifurcation cascade until attaining the fixed point $\Theta = -p/qa^*$ at $p \simeq 0.157$ (for $q = 1$). At this point, coexisting with the stable fixed point, a chaotic attractor and its basin of attraction are created around the jump vertex located at $\Theta \simeq 1$ and $a = p$, as can be seen in figure 3. Thus, depending on the initial condition, the dynamics may lead the system to one of the two attractors. The chaotic attractor appears when its basin of attraction and the stable manifold of the fixed point $\Theta = -p/qa^*$ stop overlapping. The basin of attraction is shown in figure 4 for $p = 0.2$ and presents a very complex structure, although not a fractal. In the case shown the basin of attraction is disjoint and presents at least one interior region

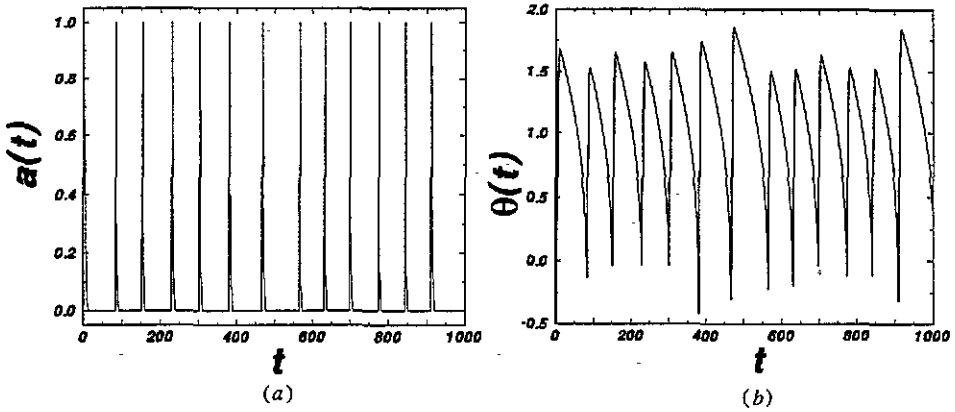


Figure 5. The threshold and the activity as a function of time for $p = 0.02$ and $q = 1$ showing the intermittent behaviour.

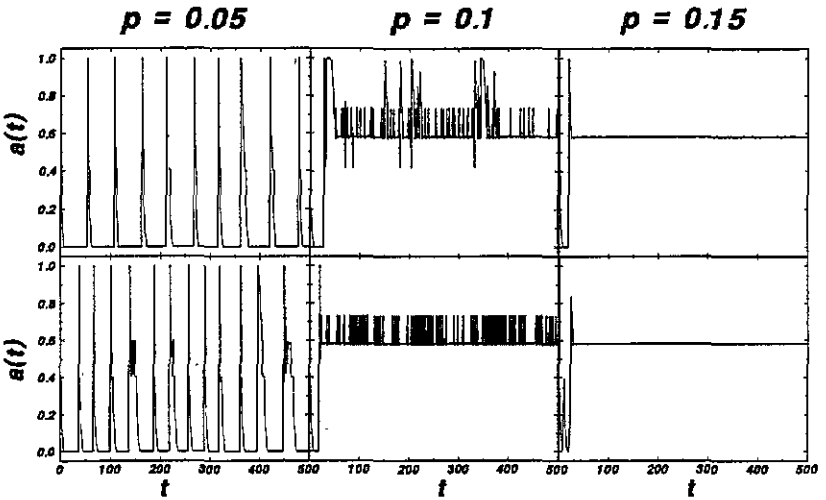


Figure 6. The solution of equation(7) versus t (bottom) along with the result of numerical simulation for $N = 30\,000$ and several values of p ($q = 1$) (top). The initial values of θ and a were $a(0) = 0.5$ and $\theta(0) = 0.9$.

that launches the system into the basin of the fixed point. An interesting feature is that an orbit starting inside one of the boundary fingers is mapped in all other fingers located at its left. For $p < 0.157$, still in the intermittent regime, the system presents a chaotic transient in the region formerly occupied by the chaotic attractor.

For $p = 0$ the system stabilizes at any point where $\Theta > C$ and $a = 0$. When $p > 0$, the p -term and q -term in the threshold map (equation (1)) compete and points with $\Theta > C$ are not stable anymore. For $0 < p < p_c \simeq 0.054$, the intermittency develops as follows: when Θ is large, a is zero and Θ slowly diminishes to small values, when it suffers a fast decrease, turns $a = 1$ and becomes large again in the following time step. This behaviour is clearly intermittent and not periodic, as it can be seen from figure 5.

The above analytical results can be successfully compared with numerical simulations even without the use of exponentially large networks [8] as shown in figure 6. The

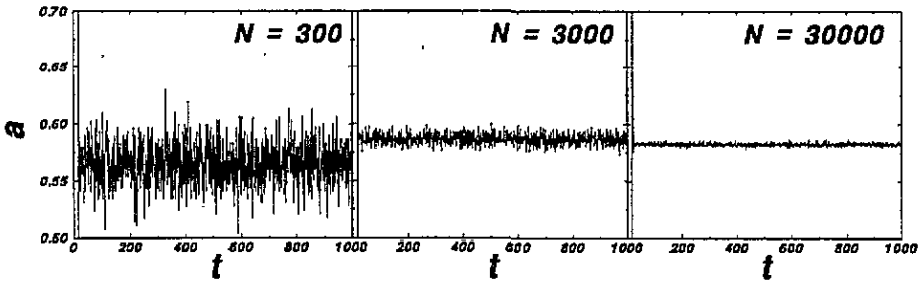


Figure 7. The activity a versus t for several values of N . The fluctuations can be seen to decrease as the network size increases. The parameters are $p = 0.15$ and $q = 1$.

simulation was performed using network sizes up to $N = 30\,000$ in contrast with [6] where only 300 neurons were utilized. Each neuron is connected to another randomly chosen 10 neurons. In figure 7 the white noise identified in [6] as signalling chaos is actually a finite-size effect: its amplitude decreases as the samples size increase. On the other hand, the intermittent behaviour, also found by Moreira and Auto, does not disappear when larger networks are considered. In figure 6 we compare the results from simulation with the analytical ones for several values of p showing the very good agreement between them.

4. Conclusions

In summary, we considered a recently proposed model for a dynamical system of coupled neurons with variable thresholds. We solved the model analytically and compared the results with numerical simulation. We introduced the notion of a jump vertex in discontinuous maps, generalizing the concept that appears in continuous flows.

Besides the usual appearance of a chaotic attractor through a doubling period route, the system also presents another chaotic attractor around a jump vertex (for some range of p) that coexists with the stable fixed point. This chaotic attractor is destroyed several times due to the collision with the basin of attraction of the stable fixed point. Just after these crises occur, the system presents a chaotic transient in the region previously occupied by the former stable chaotic attractor. The first chaotic attractor is also destroyed in an interior crisis when it collides with the unstable fixed point. Below this value of p , there is no stable attractor of the dynamics and there is an intermittent behaviour in the activity. These results were also confirmed by numerical simulation.

The same techniques can be applied for a model with learning and the effects of loading and different rules for the dynamical thresholds can be analysed. It would be interesting to investigate the role of asymmetric dilution studying either the fully connected model or a version with symmetric dilution.

Acknowledgments

We are in debt with L G Brunnet for helpful discussions and J R Iglesias for encouraging this work. The research was partially supported by Brazilian agencies CNPq, FINEP and FAPERGS.

References

- [1] Skarda C A and Freeman W J 1987 *Behavioral Brain Sciences* **10** 161
- [2] Lemke N, Arenzon J J and Tamarit F A 1994 submitted
- [3] Parisi G 1986 *J. Phys. A: Math. Gen. A* **19** L675
- [4] For a review see Kuhn R and van Hemmen J L *Physics of Neural Networks* ed E Domany, J L van Hemmen and K Schulten (Berlin: Springer) 1990
- [5] Horn D and Usher M 1989 *Phys. Rev. A* **40** 1036
Horn D 1993 *Physica* **200A** 594 and references therein
- [6] Moreira J E and Auto D M 1993 *Europhys. Lett.* **21** 639
- [7] Derrida B, Gardner E and Zippelius A 1987 *Europhys. Lett.* **4** 167
- [8] Arenzon J J and Lemke N 1994 *J. Phys. A: Math. Gen.* **27** 5161
- [9] Hirsch M W and Smale S 1974 *Differential Equations, Dynamical Systems and Linear Algebra* (New York: Academic)
- [10] Grebogi C, Ott E and Yorke J A 1982 *Phys. Rev. Lett.* **22** 1507
- [11] Grebogi C, Ott E and Yorke J A 1983 *Physica* **7D** 181